

luminosity.

The large angle bremsstrahlung is essentially the same process as the small angle one. The bremsstrahlung cross section being peaked very forward, is still sizeable at large angles. Assuming that both, electron and photon have energy above 1 GeV and are observable in the Rear Calorimeter of ZEUS (4° to 60° to the electron beam) the estimated cross section is ~ 2.3 nb. Observation of bremsstrahlung at large angles has some experimental advantages. The two serious problems at small angles, gas bremsstrahlung and synchrotron radiation should be much less annoying. Although the cross section is bigger, than that for $ep \rightarrow e\mu^+\mu^-$, it suffers from the same problem, uncertainty from the inelastic channel, which may even prevail over the elastic one in this case [52]. The large angle bremsstrahlung can serve as another cross check for the integrated luminosity measurement.

Comparing all the discussed processes, it can be concluded that the small angle bremsstrahlung process seems to be most promising for fast luminosity measurement, although the other processes can still be useful as cross checks.

1.5 Summary

Determination of luminosity for ZEUS experiment has to be based on a measurement of an event rate R of a suitably chosen process with a well known cross section σ and calculated according to the relation $L = R/\sigma$.

Requirements set to the process put in favour the small angle bremsstrahlung as the best candidate for fast luminosity monitoring. Geometry of the HERA ring allows for detection of this process with high efficiency.

Chapter 2

Bremsstrahlung

Bremsstrahlung during collisions of electron and proton bunches in HERA can be obviously described as a result of many elementary electron-proton bremsstrahlung processes $ep \rightarrow e\gamma$ (EPB). Interactions of the electrons with the rest gas atoms lead to the electron-gas bremsstrahlung (EGB), which is expected to be the main contribution to background.

The bremsstrahlung process has a very attractive feature: photons are emitted in the forward direction. To get a feeling of it, imagine a sniper, who is shooting at a coin, 34 mm in diameter from the distance of 1 kilometer, and hitting it 50 times per 100 shots. Such an excellent sniper is the Nature and Her gun - the bremsstrahlung process at HERA.

A comprehensive review of the bremsstrahlung cross section formulae can be found in [33]. Calculations for HERA, using modern methods, have been performed in [34].

2.1 Differential cross section

The lowest order Feynman diagrams for the EPB are shown in Figure 2.1. Calculations of the matrix element for bremsstrahlung on the target of charge Z in the Born approximation, for the extreme relativistic case $E \gg m$, $E' \gg m$ lead to the differential cross section, which at small angles has the form [38]

$$d\sigma = \frac{8Z^2\alpha r_e^2}{\pi} \frac{dk}{k} \frac{E'm^4}{Eq^4} \delta\delta' d\delta d\delta' d\phi \times \\ \left[\frac{\delta^2}{(1+\delta^2)^2} + \frac{\delta'^2}{(1+\delta'^2)^2} + \frac{k^2}{2EE'} \frac{\delta^2 + \delta'^2}{(1+\delta^2)(1+\delta'^2)} - \right]$$

$$\left(\frac{E'}{E} + \frac{E}{E'} \right) \frac{\delta \delta' \cos \phi}{(1 + \delta^2)(1 + \delta'^2)} \Bigg], \quad (2.1)$$

with

$$\delta = \frac{E}{m} \theta, \quad \delta' = \frac{E'}{m} \theta', \quad (2.2)$$

where:

k = photon energy,

E, E' = primary and secondary electron energy,

θ, θ' = primary and secondary electron angle (to photon),

ϕ = azimuthal angle between primary and secondary electrons,

m = electron mass

α = fine structure constant

α = fine structure constant,
 r_e = classical radius of electron

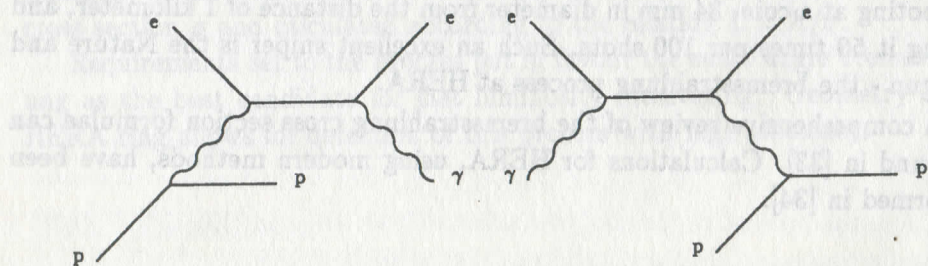


Figure 2.1: Feynman diagrams for the electron-proton bremsstrahlung.

The square of the momentum transfer to the target is

$$q^2 = m^2 \left[(\delta^2 + \delta'^2 - 2\delta\delta' \cos\phi) + m^2 \left(\frac{1+\delta^2}{2E} - \frac{1+\delta'^2}{2E'} \right)^2 \right]. \quad (2.3)$$

The target particle plays a role of a source of the Coulomb field only, so its internal structure is disregarded. Besides, in this approximation the cross section is identical for electrons and positrons.

22. BETHE-HEITLER FORMULA

2.2 Bethe-Heitler formula

Integration of (2.1) over the angles leads to the famous Bethe-Heitler formula [35, 36], which in case of $Z = 1$ reads:

$$\frac{d\sigma}{dk} = 4\alpha r_e^2 \frac{E'}{kE} \left(\frac{E}{E'} + \frac{E'}{E} - \frac{2}{3} \right) \left(\ln \frac{2EE'}{mk} - \frac{1}{2} \right) \quad (2.4)$$

The maximum photon energy is $k_{max} = (1 - m^2/E^2)E$. The hard end of the photon spectrum is not well reproduced by formula (2.4), but it can be applied up to $k \leq E - m$ giving accuracy sufficient for luminosity purposes. It follows from (2.3), that the maximum momentum transfer to the proton $q_{max} \simeq m$, therefore the energy transfer $\Delta E \leq \frac{m^2}{2M} \simeq 1 \cdot 10^{-4} MeV$ is negligible and

$$E' \equiv E - k, \quad (2.5)$$

The formula (2.4) assumes the proton at rest, so it can be applied to EPB at HERA in the proton beam frame. In order to transform it to the laboratory frame, one has to use the Lorentz transformation, which in case of high energies ($\gg m$) and small angles ($\sim m/E$) takes the very simple form:

$$\begin{aligned} E &\rightarrow 2\gamma E \\ E' &\rightarrow 2\gamma E' \\ k &\rightarrow 2\gamma k \end{aligned} \quad (2.6)$$

where:

$$\gamma = E_p/M$$

$E_p \equiv$ proton energy

M = proton mass

After the transformation (2.4) reads:

$$\frac{d\sigma}{dk} = 4\alpha r_e^2 \frac{E'}{kE} \left(\frac{E}{E'} + \frac{E'}{E} - \frac{2}{3} \right) \left(\ln \frac{4E_p E E'}{M m k} - \frac{1}{2} \right) \quad (2.7)$$

One can observe that only the logarithmic term has changed. Figure 2.2 shows the photon spectra according to (2.7) for some values of E and E_p . At low photon energy all the spectra show identical, classical k^{-1} behaviour. The second plot presenting the spectra using the variable k/E instead of k , demonstrates that shape of the photon spectrum is practically independent on the electron and proton beam energies. Similar behaviour show also angular distributions of the bremsstrahlung. This allows to restrict most of considerations to the

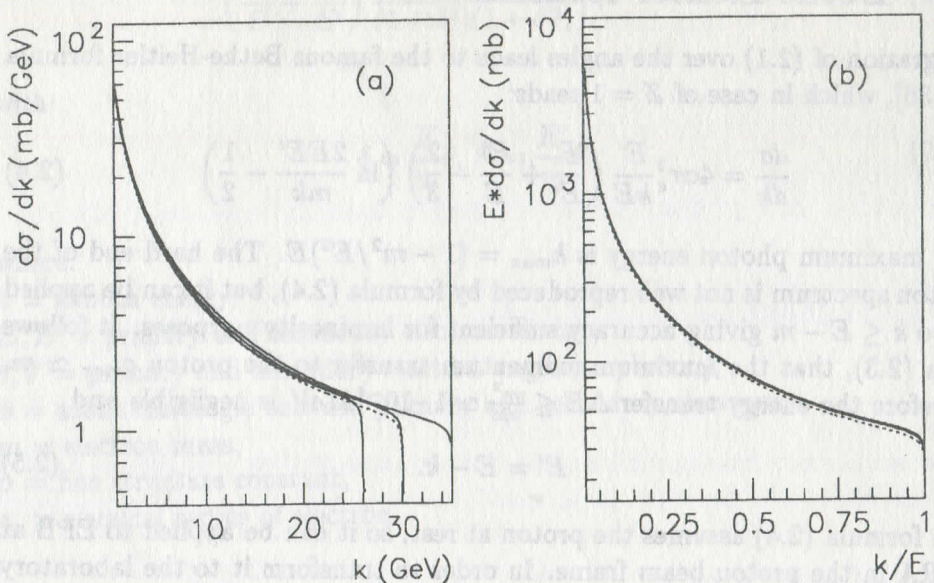


Figure 2.2: a. Photon spectra of EPB for $E_p = 820$ GeV and $E = 26, 30, 35$ GeV (solid lines) and for $E_p = 300$ GeV and $E = 30$ GeV (dotted line). b. Photon spectra as before, but using k/E as abscissa.

standard HERA energies $E_p = 820$ GeV and $E = 30$ GeV. These values will be assumed in the following, if not marked otherwise.

In view of (2.5), the electron spectra are trivial reflections of the photon spectra.

2.3 Angular distributions

Angular distribution of EPB photons has been calculated in [37], but more convenient for discussion is the extremely relativistic limit [38]. After the necessary Lorentz transformation, performed using (2.6), the differential cross section reads:

$$\frac{d\sigma}{d\delta dk} = 8\alpha r_e^2 \frac{E'}{kE} \frac{\delta}{(1+\delta^2)^2} \left\{ \left[\frac{E}{E'} + \frac{E'}{E} - \frac{4\delta^2}{(1+\delta^2)^2} \right] \ln \frac{4E_p EE'}{Mmk} - \frac{1}{2} \left[\frac{E}{E'} + \frac{E'}{E} + 2 - \frac{16\delta^2}{(1+\delta^2)^2} \right] \right\} \quad (2.8)$$

2.3. ANGULAR DISTRIBUTIONS

The photon angular distribution is almost independent of the photon energy. This is demonstrated in Figure 2.3a, where the probability density, calculated as a ratio of (2.8) to (2.7) is plotted. In a good approximation

$$\frac{d\sigma}{d\theta} \sim \frac{\theta}{(\theta_0^2 + \theta^2)^2}, \quad (2.9)$$

where $\theta_0 = m/E$.

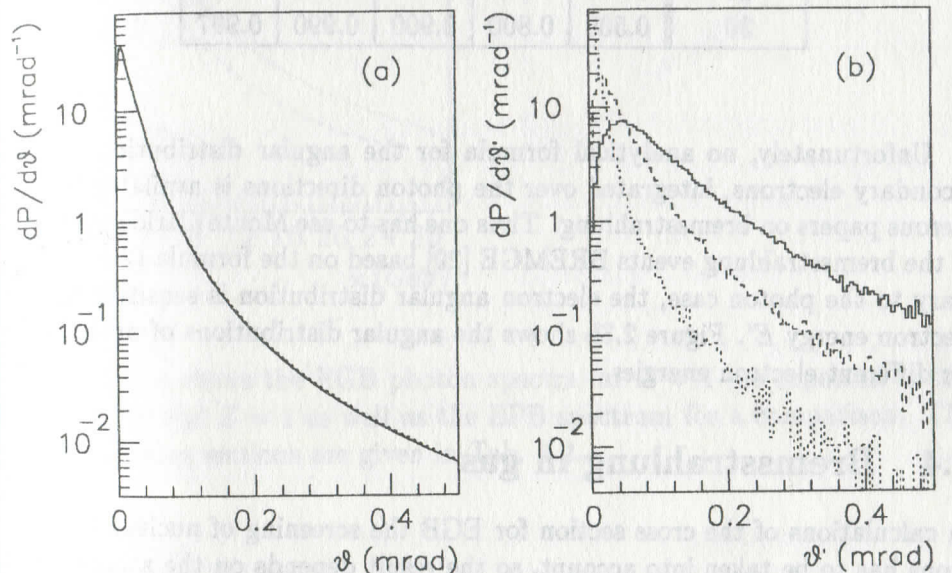


Figure 2.3: a. Photon angle θ probability distribution for two photon energies: 10 GeV (solid line) and 0.1 GeV (dotted line), b. Electron angle θ' probability distribution for three electron energies: 5 GeV (solid line), 10 GeV (dashed line) and 20 GeV (dotted line).

The parameter θ_0 ($\theta_0 = 17 \cdot 10^{-6}$ rd at $E = 30$ GeV) is the 'natural' unit for the photon emission angle. It is easy to show that θ_0 equals to the median $\theta_{1/2}$ of the distribution, ie. exactly 50% of photons (of any energy) are emitted at angles $\theta \leq \theta_0$. One can also calculate the mean photon angle

$$\bar{\theta}(k) = \frac{\pi}{2} \theta_0 w\left(\frac{k}{E}\right), \quad (2.10)$$

where $w\left(\frac{k}{E}\right) \simeq 1$ is a slowly varying function over the whole range of photon energy ($w(0) = 9/8$, $w(1) = 1$). Table 2.1 gives the cumulated angular distributions at three photon energies.

Table 2.1: Probability that the bremsstrahlung photon is emitted at angle less or equal θ .

| k (GeV) | θ (mrad) | | | | |
|-----------|-----------------|-------|-------|-------|-------|
| | 0.017 | 0.034 | 0.085 | 0.17 | 0.34 |
| 1 | 0.500 | 0.755 | 0.866 | 0.986 | 0.996 |
| 10 | 0.500 | 0.761 | 0.870 | 0.986 | 0.996 |
| 30 | 0.500 | 0.800 | 0.900 | 0.990 | 0.997 |

Unfortunately, no analytical formula for the angular distribution of the secondary electrons, integrated over the photon directions is available in numerous papers on bremsstrahlung. Thus one has to use Monte Carlo generator of the bremsstrahlung events BREMGE [20] based on the formula (2.1). Contrary to the photon case, the electron angular distribution is sensitive to the electron energy E' . Figure 2.3b shows the angular distributions of probability for different electron energies.

2.4 Bremsstrahlung in gas

In calculations of the cross section for EGB the screening of nucleus by electrons has to be taken into account, so the result depends on the atomic form factor used in calculations. Due to high energies and small angles involved in the process, the nucleus field is completely screened by the atomic electrons. The differential cross section in this case is [39]:

$$\frac{d\sigma}{dk} = 4\alpha r_e^2 \frac{E'}{kE} \left[\left(\frac{E}{E'} + \frac{E'}{E} - \frac{2}{3} \right) (Z^2 L_{rad} + Z L'_{rad}) + \frac{1}{9} (Z^2 + Z) \right] \quad (2.11)$$

where: L_{rad} and L'_{rad} , called 'radiation logarithms' are functions of the atomic form factor. If the Fermi-Thomas-Moliere model is used [40, 41], then

$$\begin{aligned} L_{rad} &= \ln(184Z^{-1/3}) \\ L'_{rad} &= \ln(1194Z^{-2/3}). \end{aligned} \quad (2.12)$$

Terms in (2.11) proportional to Z^2 account for the bremsstrahlung from the nucleus, while the terms proportional to Z give the contribution from atomic electrons. Since L_{rad} and L'_{rad} are of the same order of magnitude and vary slowly with Z , the EGB cross section is roughly proportional to $Z^2 + Z$.

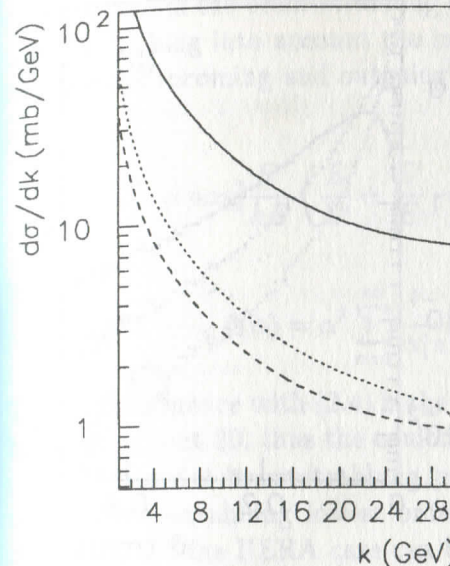


Figure 2.4: Photon spectra of EGB for $Z = 4$ (solid line), $Z = 1$ (dashed line) and EPB (dotted line).

Figure 2.4 shows the EGB photon spectra for $Z = 4$ (as expected in the HERA ring) and $Z = 1$ as well as the EPB spectrum for a comparison. The integrated cross sections are given in Tab. 2.2.

Table 2.2: Integrated cross sections for e-p and e-gas ($Z = 4$) bremsstrahlung ($E=30$ GeV).

| σ (mb) | k (GeV) | | | | |
|------------------|-----------|-------|--------|---------|---------|
| | 1 - 4 | 4 - 8 | 8 - 14 | 14 - 20 | 20 - 30 |
| e - p | 85.0 | 36.1 | 24.6 | 13.7 | 14.3 |
| e-gas | 408.8 | 183.4 | 103.9 | 76.0 | 87.6 |

The angular distributions of photons and electrons are very similar to those for EPB. They have been calculated using Monte Carlo generator BREMGE and are shown in Figure 2.5. Broadening of the angular distributions as the result of screening is clearly seen.

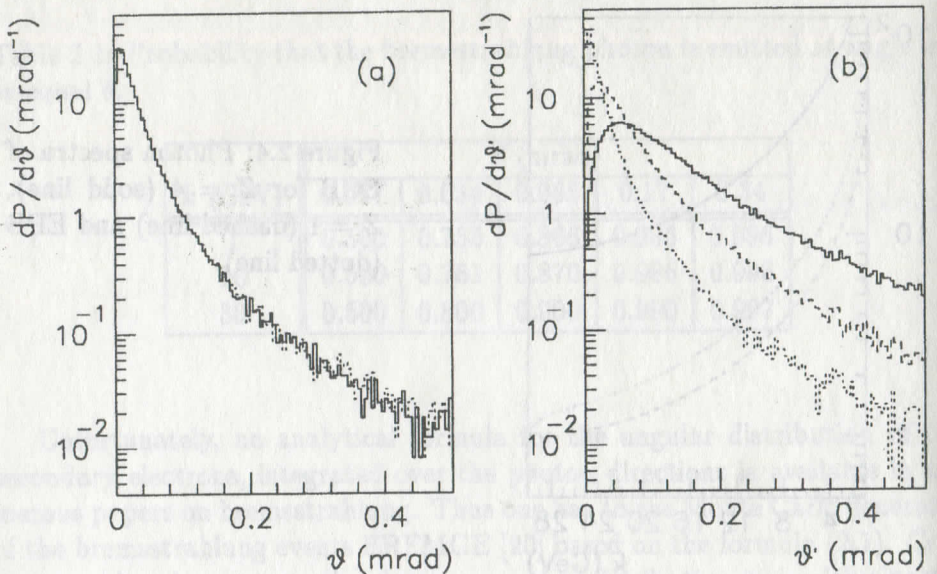


Figure 2.5: Angular distributions in EGB for: a. Photons of energy $k = 20$ GeV (solid line), 10 GeV (dashed line) and 0.1 GeV (dotted line), b. Electrons of energy $E' = 20$ GeV (solid line), 10 GeV (dashed line) and 5 GeV (dotted line).

2.5 Corrections

Now one has to discuss a question, how accurate are the theoretical results presented in previous sections. Much of attention will be paid to the evaluation of the EPB cross section, which is essential for the luminosity monitoring. Since the corrections to the cross section are generally small, their influence on EGB will not be considered. The list of points to discuss is the following:

- Coulomb wave functions,
- higher order processes,
- inelastic processes,
- beam-size effect,
- coherence length effect,
- beamstrahlung,

Z^0 exchange.

Calculations of the bremsstrahlung cross section without the Born approximation, i.e. taking into account the influence of the Coulomb field on the wave functions of incoming and outgoing electrons gives the following cross section [38]:

$$\frac{d\sigma}{dk} = 4\alpha r_e^2 \frac{E'}{kE} \left(\frac{E}{E'} + \frac{E'}{E} - \frac{2}{3} \right) \left(\ln \frac{2EE'}{mk} - \frac{1}{2} - f(\alpha) \right) \quad (2.13)$$

where

$$f(\alpha) = \alpha^2 \sum_{n=1}^{\infty} \frac{1}{n(n^2 + \alpha^2)} \simeq 1.2\alpha^2 \simeq 6 \cdot 10^{-5} \quad (2.14)$$

The only difference with (2.4) is the term $f(\alpha)$. The logarithmic term in (2.13) has value about 20, thus the coulomb correction is found to be negligible.

Higher order bremsstrahlung processes play role of radiative corrections to the bremsstrahlung lowest order process. The detailed calculations and discussion for the HERA case can be found in [42]. The radiative corrections can be divided into two parts depending on the γ -detector energy resolution E_{soft} :

1. emission of a hard photon ($E'_\gamma > E_{soft}$) and
2. emission of soft ($E'_\gamma < E_{soft}$) and virtual photons.

In the case (1) it is assumed that both emitted photons are detected but cannot be resolved, in the case (2) – only one, hard photon is detected.

In [42] both types of corrections were calculated for the photon energy interval 8 to 14 GeV, where the Bethe-Heitler cross section $\sigma_{BH} \simeq 25$ mb. For $E_{soft} = 0.1$ GeV $\Delta\sigma_{hard} = 0.05$ mb and $\Delta\sigma_{soft+virt} = -0.04$ mb, while for $E_{soft} = 1$ GeV $\Delta\sigma_{hard} = 0.02$ mb and $\Delta\sigma_{soft+virt} = 0.05$ mb. The energy resolution of the γ -calorimeter in the considered energy range is 0.5 to 0.7 GeV, thus the overall correction $\Delta\sigma_{rad} < 0.07$ mb $\simeq 0.3\% \cdot \sigma_{BH}$.

The inelastic process $ep \rightarrow \gamma eX$, where X is any hadronic state, may give rise to the bremsstrahlung process if X cannot be detected because of small angles of produced hadrons. The upper limit for the inelastic cross section has been calculated in [43] and amounts to only 0.16 μb .

The beam size effect is a new phenomenon, specific for high energy colliders, where interacting particles are confined to bunches of small transverse dimensions. A simplified explanation of the effect is based on the well known fact that most of the bremsstrahlung cross section is connected with low values

of the momentum transfer, namely close to the minimum value, which is given by

$$q_{\min} = \frac{m^2 M k}{4 E_p E'}. \quad (2.15)$$

The transverse component of the minimum momentum transfer $q_{\min,\perp}$ corresponds to the maximum impact parameter of the collision

$$b_{\max} = \frac{\hbar c}{q_{\min,\perp}} = 0.08 m m \frac{E'}{k}. \quad (2.16)$$

On the other hand, the values of the impact parameter are evidently limited by the transverse size of the collision region \bar{r} . Thus emission of photons of energy $k \leq \frac{0.08 m m}{\bar{r}} E$ ($E' \simeq E$ for low k) should be suppressed. This phenomenon, called 'the beam-size effect', was observed in e^+e^- collider [44]. Results of calculations for HERA and for LEP are shown in Figure 2.6 taken from [45]. The overall correction in the range $k = 8 - 14$ GeV is $\Delta\sigma_{bs} \simeq -0.5\% \cdot \sigma_{BH}$.

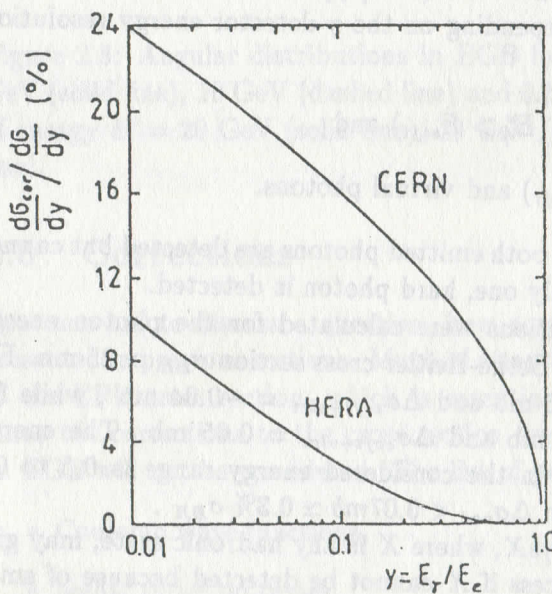


Figure 2.6: Beam size effect at HERA and LEP. Correction (%) to the Bethe-Heitler cross section is plotted as a function of photon energy to beam energy ratio.

Another mechanism of suppression of the bremsstrahlung emission is known as the Landau-Pomeranchuk effect or the coherence length effect. Landau and Pomeranchuk have pointed out [47] that the emission of a bremsstrahlung photon is performed over a distance called the coherence length and the multiple Coulomb scattering can disturb this process and suppress the photon emission.

2.6. SUMMARY

The effect has been observed in cosmic ray experiments [48, 49]. Experimental significance of the effect at HERA has been discussed [21] and the conclusion is that it could be observed, if ever, only in the low energy part of the gamma spectrum, and thus would not affect luminosity monitoring.

Recently the problem of the "super-colliders". With the increasing energy and CERN in view of the future, incoming electrons, they begin to interact with the opposite bunch as a whole rather than with the individual particles. This should lead to a dramatic rise of energy loss and is referred to as "beamstrahlung". However, theoretical estimates [50, 51] set the conditions for electron energy ($E \geq 1$ TeV) and beam radius ($r \ll 1\mu\text{m}$) far from the origin. influence the luminosity monitoring.

Calculations of the beamstrahlung cross section taking into account both γ and Z^0 exchange [52] show that there is no noticeable Z^0 contribution in the considered phase space region.

2.6 Summary

The process $ep \rightarrow e p \gamma$ has the following characteristics:

1. The cross section is large ($\sigma(8 \leq k \leq 14 \text{ GeV}) = 24.6 \text{ mb}$). As shown in the next chapter, the rate of the bremsstrahlung events is much larger than that of any of the competing processes.
2. The cross section is calculable from QED with a very good accuracy ($\sim 0.2\%$). The overall correction to the Bethe-Heitler cross section σ_{BH} ($k = 8 - 14 \text{ GeV}$) is $\Delta\sigma \simeq -0.2\% \cdot \sigma_{BH}$ for $k = 8 - 14 \text{ GeV}$. This correction can be easily disregarded as compared to large experimental errors, at least in the first stage of the experiment.
3. The angular distribution is peaked very forward. It enables us to obtain a high detection efficiency by using small detectors.
4. The signature of the process is clear. Detection of both final particles, the photon and the electron, is feasible and the energy conservation check can be applied.

They prove that this process fulfills the requirements for the luminosity monitoring.